

Dysprosium(III) Complexes with Square-Antiprism Configuration Featuring Mononuclear Single-molecule Magnet Behaviours Based on Different β -diketonate Ligands and Auxiliary Ligands

Sheng Zhang,^{a,d} Hongshan Ke,^a Quan Shi,^b Jangwei Zhang,^c Qi Yang,^a Qing Wei,^a Gang Xie,^a Wenyuan Wang,^a Desuo Yang,^d Sanping Chen^{*a}

^a*Key Laboratory of Synthetic and Natural Functional Molecule Chemistry of Ministry of Education, College of Chemistry and Materials Science, Northwest University, Xi'an, Shaanxi 710069, China*

^b*Dalian Institute of Chemical Physics, Chinese Academy of Sciences, 457 Zhongshan Road, Dalian 116023, China.*

^c*Department of Chemistry, Tsinghua University, Beijing 100084, China*

^d*College of Chemistry and Chemical Engineering, Baoji University of Arts and Sciences, Baoji 721013, China.*

Corresponding authors

Dr. Sanping Chen

E-mail address: sanpingchen@126.com; sanpingchen312@gmail.com

Table S1 Crystal data and structure refinement details for the complexes **1-3**.

Compound	1	2	3
Empirical formula	C45H31DyF9N3O8	C36H29DyF12N2O8	C52H33DyF9N2O6
Formula weight	1075.23	1008.11	1115.30
Temperature	296(2) K	296(2) K	296(2) K
Crystal system	Triclinic	Triclinic	Monoclinic
space group	<i>P</i> -1	<i>P</i> -1	<i>P</i> 2/c
<i>a</i> (Å)	10.035(7)	11.2264(15)	22.748(6)
<i>b</i> (Å)	13.495(9)	13.5298(17)	10.942(3)
<i>c</i> (Å)	16.844(12)	14.1233(18)	21.315(5)
α (°)	93.993(15)	94.868(2)	90
β (°)	91.198(14)	101.031(2)	108.438(6)
γ (°)	94.372(14)	102.060(2)	90
<i>V</i> (Å ³)	2268(3)	2041.6(5)	5033(2)
<i>Z</i>	2	2	4
F(000)	1066	1066	2216
Goodness-of-fit on F ²	0.956	0.941	1.036
Final <i>R</i> indices [<i>I</i> >2sigma(<i>I</i>)]	<i>R</i> ₁ = 0.0963 <i>wR</i> ₂ = 0.1244	<i>R</i> ₁ = 0.0463 <i>wR</i> ₂ = 0.1251	<i>R</i> ₁ = 0.0590 <i>wR</i> ₂ = 0.1358
<i>R</i> indices (all data)	<i>R</i> ₁ = 0.3406 <i>wR</i> ₂ = 0.1831	<i>R</i> ₁ = 0.0613 <i>wR</i> ₂ = 0.1462	<i>R</i> ₁ = 0.1265 <i>wR</i> ₂ = 0.1741
CCDC	1438720	1444533	1444532

Table S2. Selected bond lengths (Å) and angles (°) for **1-3**.

1			
Dy(1)-O(4)	2.255(12)	O(4)-Dy(1)-O(6)	77.5(4)
Dy(1)-O(1)	2.269(12)	O(1)-Dy(1)-O(6)	150.1(4)
Dy(1)-O(5)	2.275(11)	O(5)-Dy(1)-O(6)	73.1(4)
Dy(1)-O(3)	2.297(11)	O(3)-Dy(1)-O(6)	116.5(4)
Dy(1)-O(2)	2.325(11)	O(2)-Dy(1)-O(6)	81.9(4)
Dy(1)-O(6)	2.333(12)	O(4)-Dy(1)-N(2)	145.4(5)
Dy(1)-N(2)	2.473(14)	O(1)-Dy(1)-N(2)	107.6(4)
Dy(1)-N(1)	2.570(16)	O(5)-Dy(1)-N(2)	77.4(4)
O(4)-Dy(1)-O(1)	81.4(4)	O(3)-Dy(1)-N(2)	140.8(5)
O(4)-Dy(1)-O(5)	119.4(4)	O(2)-Dy(1)-N(2)	73.9(4)
O(1)-Dy(1)-O(5)	136.5(4)	O(6)-Dy(1)-N(2)	79.8(4)
O(4)-Dy(1)-O(3)	73.4(4)	O(4)-Dy(1)-N(1)	148.4(4)
O(1)-Dy(1)-O(3)	76.5(4)	O(1)-Dy(1)-N(1)	72.3(4)
O(5)-Dy(1)-O(3)	74.5(4)	O(5)-Dy(1)-N(1)	72.8(4)
O(4)-Dy(1)-O(2)	77.3(4)	O(3)-Dy(1)-N(1)	83.5(5)
O(1)-Dy(1)-O(2)	72.9(4)	O(2)-Dy(1)-N(1)	110.1(4)
O(5)-Dy(1)-O(2)	144.8(4)	O(6)-Dy(1)-N(1)	133.3(4)

O(3)-Dy(1)-O(2)	140.2(4)	N(2)-Dy(1)-N(1)	62.3(5)
-----------------	----------	-----------------	---------

2			
Dy(1)-O(5)	2.311(4)	O(5)-Dy(1)-O(3)	144.39(17)
Dy(1)-O(1)	2.335(4)	O(1)-Dy(1)-O(3)	75.54(17)
Dy(1)-O(2)	2.335(4)	O(2)-Dy(1)-O(3)	74.45(16)
Dy(1)-O(4)	2.343(4)	O(4)-Dy(1)-O(3)	71.51(15)
Dy(1)-O(6)	2.356(4)	O(6)-Dy(1)-O(3)	122.77(15)
Dy(1)-O(3)	2.360(4)	O(5)-Dy(1)-O(7)	140.52(17)
Dy(1)-O(7)	2.388(5)	O(1)-Dy(1)-O(7)	144.30(16)
Dy(1)-O(8)	2.400(5)	O(2)-Dy(1)-O(7)	81.28(16)
O(5)-Dy(1)-O(1)	73.15(15)	O(4)-Dy(1)-O(7)	106.18(17)
O(5)-Dy(1)-O(2)	111.01(15)	O(6)-Dy(1)-O(7)	74.97(16)
O(1)-Dy(1)-O(2)	72.45(15)	O(3)-Dy(1)-O(7)	74.38(17)
O(5)-Dy(1)-O(4)	87.49(16)	O(5)-Dy(1)-O(8)	71.50(18)
O(1)-Dy(1)-O(4)	81.74(16)	O(1)-Dy(1)-O(8)	116.15(18)
O(2)-Dy(1)-O(4)	141.35(16)	O(2)-Dy(1)-O(8)	73.20(17)
O(5)-Dy(1)-O(6)	74.38(14)	O(4)-Dy(1)-O(8)	145.29(17)
O(1)-Dy(1)-O(6)	138.95(15)	O(6)-Dy(1)-O(8)	75.43(17)
O(2)-Dy(1)-O(6)	144.03(16)	O(3)-Dy(1)-O(8)	139.47(17)
O(4)-Dy(1)-O(6)	72.39(15)	O(7)-Dy(1)-O(8)	77.18(19)

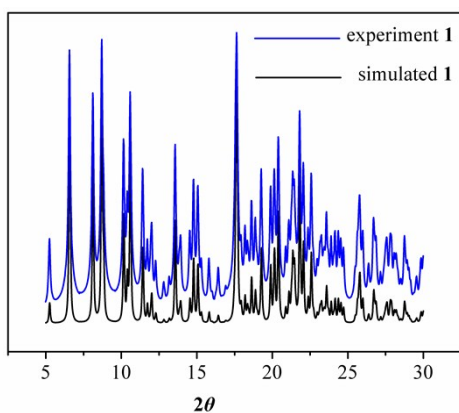
3			
Dy(1)-O(6)	2.331(16)	O(1)-Dy(1)-O(5)	147.4(5)
Dy(1)-O(5)	2.323(14)	O(1)-Dy(1)-O(2)	71.2(5)
Dy(1)-O(2)	2.361(18)	O(1)-Dy(1)-O(4)	74.0(5)
Dy(1)-O(1)	2.285(16)	O(1)-Dy(1)-N(1)	133.9(5)
Dy(1)-O(4)	2.314(12)	O(1)-Dy(1)-O(3)	115.8(6)
Dy(1)-N(1)	2.53(2)	O(1)-Dy(1)-N(2)	80.5(6)
Dy(1)-O(3)	2.284(16)	O(4)-Dy(1)-O(6)	75.1(6)
Dy(1)-N(2)	2.491(16)	O(4)-Dy(1)-O(5)	82.8(5)
O(6)-Dy(1)-O(2)	139.9(6)	O(4)-Dy(1)-O(2)	118.3(6)
O(6)-Dy(1)-N(1)	117.7(7)	O(4)-Dy(1)-N(1)	149.5(6)
O(6)-Dy(1)-N(2)	74.6(6)	O(4)-Dy(1)-N(2)	143.7(6)
O(5)-Dy(1)-O(6)	74.2(5)	O(3)-Dy(1)-O(6)	141.4(6)
O(5)-Dy(1)-O(2)	141.2(6)	O(3)-Dy(1)-O(5)	78.5(6)
O(5)-Dy(1)-N(1)	75.4(5)	O(3)-Dy(1)-O(2)	76.8(6)
O(5)-Dy(1)-N(2)	107.5(5)	O(3)-Dy(1)-O(4)	74.9(5)
O(2)-Dy(1)-N(1)	71.2(6)	O(3)-Dy(1)-N(1)	80.0(7)
O(2)-Dy(1)-N(2)	75.6(6)	O(3)-Dy(1)-N(2)	140.7(6)
O(1)-Dy(1)-O(6)	77.9(5)	N(2)-Dy(1)-N(1)	64.9(7)

Table S3 Relevant structural parameters in square anti-prism geometry, α angle

α angle ($^{\circ}$)	1	α angle ($^{\circ}$)	2	α angle ($^{\circ}$)	3
O1	58.929	O1	58.327	O1	55.067
O2	60.457	O2	56.205	O2	59.934
N1	54.085	O3	60.904	O3	57.782
N2	53.303	O4	51.067	O4	56.050
O3	55.990	O5	55.001	O5	57.267
O4	55.556	O6	61.735	O6	62.823
O5	59.278	O7	54.997	N1	57.548
O6	56.061	O8	58.007	N2	52.570
Deviation	56.707	Deviation	57.030	Deviation	57.380
Sum of deviation to ideal 54.74°	1.967	Sum of deviation to ideal 54.74°	2.290	Sum of deviation to ideal 54.74°	2.640

Table S4 Relevant structural parameters in square anti-prism geometry, ϕ angle

ϕ angle ($^{\circ}$)	1	ϕ angle ($^{\circ}$)	1	ϕ angle ($^{\circ}$)	1
O1-Dy-O3	42.928	O1-Dy-O4	43.507	O4-Dy-O6	42.322
O1-Dy-O4	46.642	O5-Dy-O4	47.793	O5-Dy-O4	47.042
O2-Dy-O4	45.814	O1-Dy-O3	43.651	O3-Dy-O5	45.378
O2-Dy-O6	47.880	O2-Dy-O3	43.725	O3-Dy-N1	46.268
N2-Dy-O6	45.871	O7-Dy-O2	47.124	N1-Dy-O2	39.224
N2-Dy-O5	44.923	O7-Dy-O8	43.562	N2-Dy-O2	42.959
N1-Dy-O3	49.909	O5-Dy-O6	43.022	O1-Dy-O6	44.674
N1-Dy-O5	42.702	O8-Dy-O6	43.476	N1-Dy-O2	47.034
Deviation	45.834	Deviation	44.483	Deviation	44.363
Sum of deviation to ideal 45°	0.834	Sum of deviation to ideal 45°	0.518	Sum of deviation to ideal 45°	0.637

Figure S1. XRPD curve of **1**.

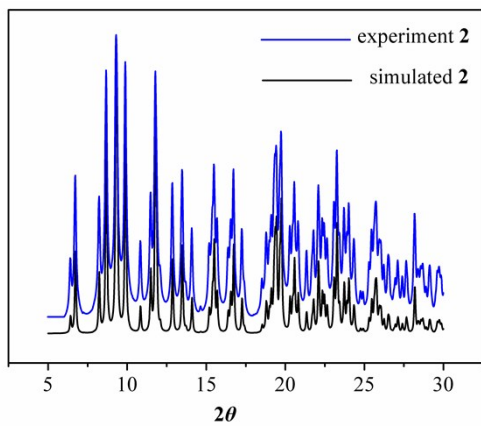


Figure S2. XRPD curve of **2**.

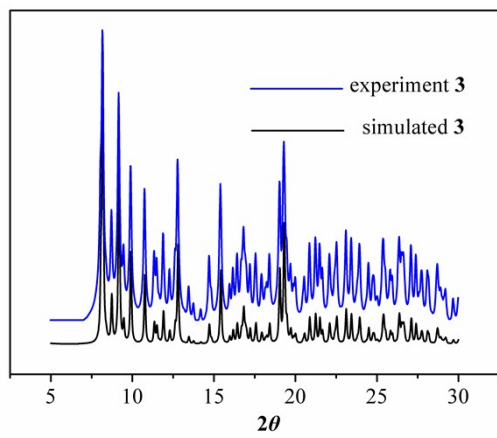
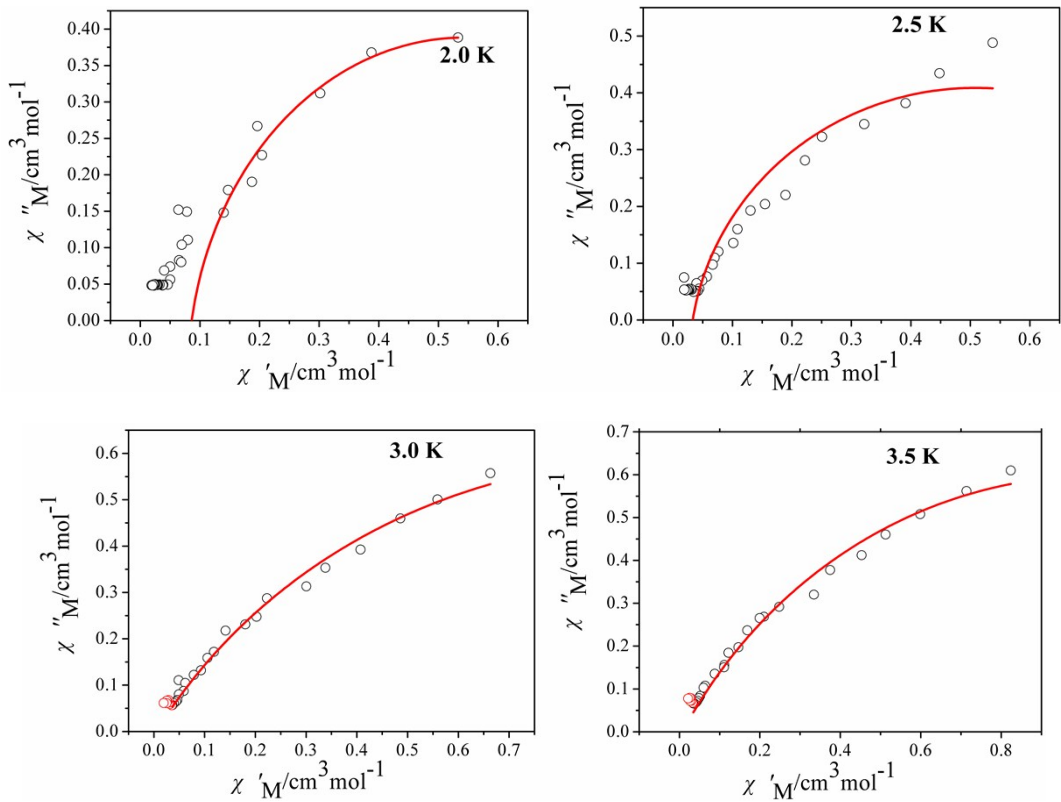
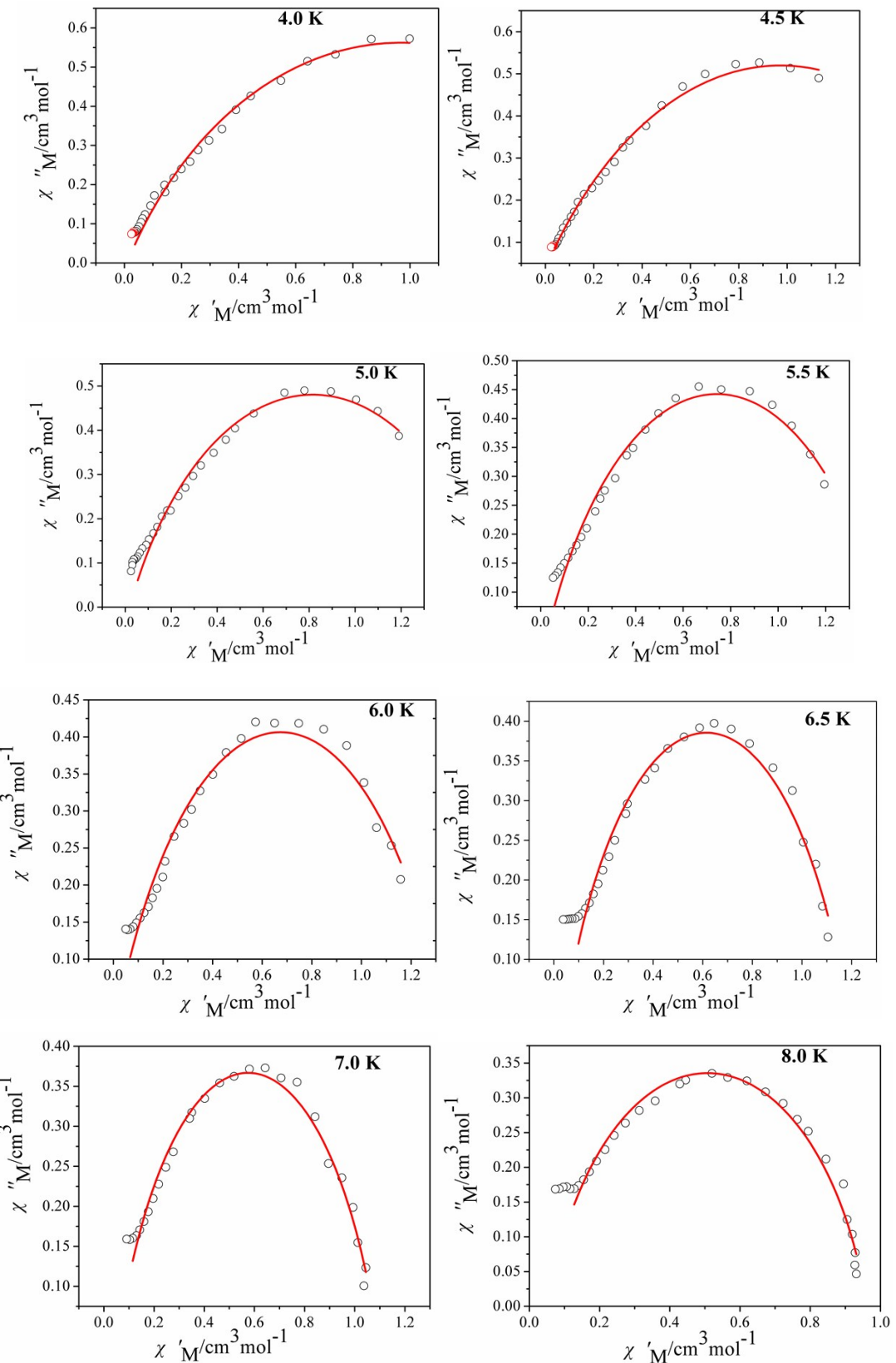


Figure S3. XRPD curve of **3**.





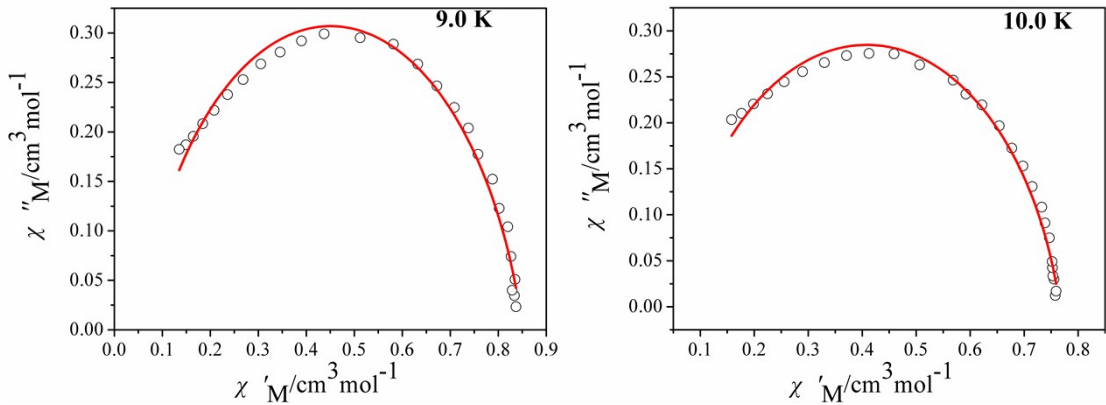


Figure S4. Simulations of dynamical susceptibility $\chi(\omega)$ ranging from 2.0 to 10 K in a Cole-Cole diagram of **1**. Red lines were performed using the sum of two modified Debye functions with the fitting parameters in Table S3. The magnetic susceptibility data were described by the modified Debye functions:

$$\chi'(\omega) = \chi_s + (\chi_t - \chi_s) \frac{1 + (\omega\tau)^{1-\alpha} \sin(\frac{\pi}{2}\alpha)}{1 + 2(\omega\tau)^{1-\alpha} \sin(\frac{\pi}{2}\alpha) + (\omega\tau)^{(2-2\alpha)}}$$

$$\chi''(\omega) = (\chi_t - \chi_s) \frac{(\omega\tau)^{1-\alpha} \cos(\frac{\pi}{2}\alpha)}{1 + 2(\omega\tau)^{1-\alpha} \sin(\frac{\pi}{2}\alpha) + (\omega\tau)^{(2-2\alpha)}}$$

$$\chi''_{\omega=\tau^{-1}} = (\chi_t - \chi_s) \frac{\cos(\frac{\pi}{2}\alpha)}{2 + 2 \sin(\frac{\pi}{2}\alpha)} = \frac{1}{2} (\chi_t - \chi_s) \tan \frac{\pi}{4} (1 - \alpha)$$

Table S5. Relaxation fitting parameters from Least-Squares Fitting of $\chi(\omega)$ data of **1**.

T(K)	$\Delta\chi_1$ (cm ³ mol ⁻¹)	$\Delta\chi_2$ (cm ³ mol ⁻¹)	α_1
2.0	2.234	0.002	0.221
2.5	2.112	0.004	0.243
3.0	2.002	0.005	0.325
3.5	2.064	0.008	0.330
4.0	1.930	0.009	0.325
4.5	1.774	0.011	0.310
5.0	1.613	0.019	0.309
5.5	1.471	0.014	0.305
6.0	1.344	0.026	0.306
6.5	1.199	0.031	0.257
7.0	1.106	0.044	0.230
8.0	0.962	0.053	0.190
9.0	0.851	0.056	0.167
10.0	0.766	0.051	0.186

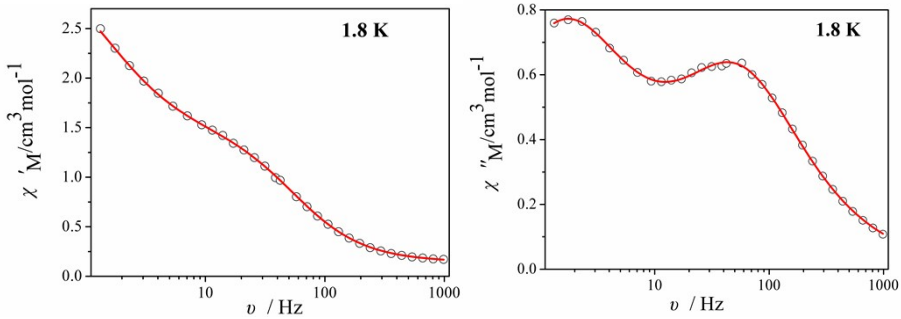


Figure S5. Frequency dependence of the in-of-phase (χ' , right) and out-of-phase (χ'' , left) ac susceptibility of **2** at 1.8 K. The full range plots can be fitted well by the following parameters: $\alpha_1 = 0.169$; $\alpha_2 = 0.126$; $\tau_1 = 2.85 \times 10^{-3}$ s; $\tau_2 = 0.104$ s; $\chi_{S,\text{tot}} = 1.322 \text{ cm}^3\text{mol}^{-1}$; $\Delta\chi_1 = 1.872 \text{ m}^3\text{mol}^{-1}$; $\Delta\chi_2 = 1.322 \text{ cm}^3\text{mol}^{-1}$. The red lines are the fits of the full range plots.

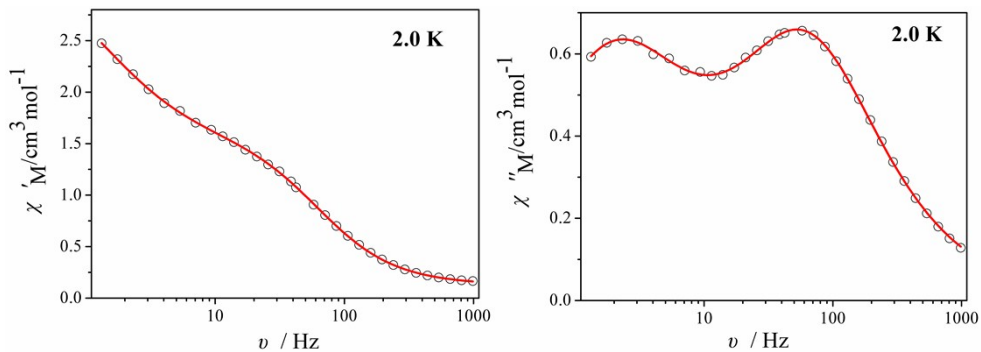


Figure S6. Frequency dependence of the in-of-phase (χ' , right) and out-of-phase (χ'' , left) ac susceptibility of **2** at 2.0 K. The full range plots can be fitted well by the following parameters: $\alpha_1 = 0.174$; $\alpha_2 = 0.13$; $\tau_1 = 2.49 \times 10^{-3}$ s; $\tau_2 = 0.084$ s; $\chi_{S,\text{tot}} = 0.122 \text{ cm}^3\text{mol}^{-1}$; $\Delta\chi_1 = 1.493 \text{ cm}^3\text{mol}^{-1}$; $\Delta\chi_2 = 1.419 \text{ cm}^3\text{mol}^{-1}$. The red lines are the fits of the full range plots.

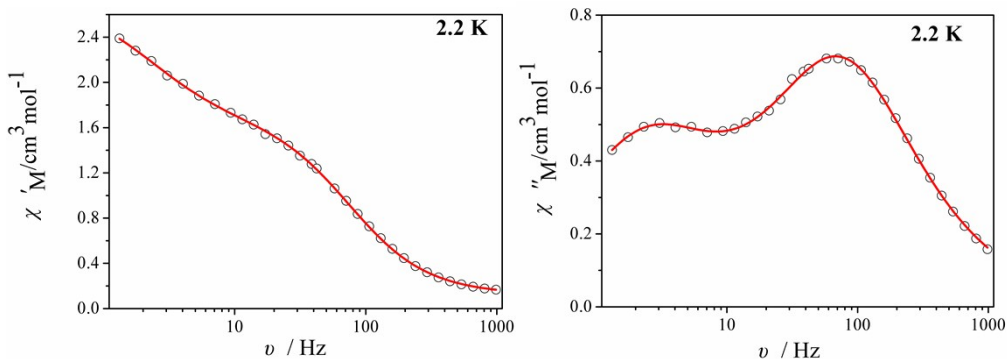


Figure S7. Frequency dependence of the in-of-phase (χ' , right) and out-of-phase (χ'' , left) ac susceptibility of **2** at 2.2 K. The full range plots can be fitted well by the following parameters: $\alpha_1 = 0.156$; $\alpha_2 = 0.131$; $\tau_1 = 2.08 \times 10^{-3}$ s; $\tau_2 = 0.069$ s; $\chi_{S,\text{tot}} = 0.115 \text{ cm}^3\text{mol}^{-1}$; $\Delta\chi_1 = 1.556 \text{ cm}^3\text{mol}^{-1}$; $\Delta\chi_2 = 1.077 \text{ cm}^3\text{mol}^{-1}$. The red lines are the fits of the full range plots.

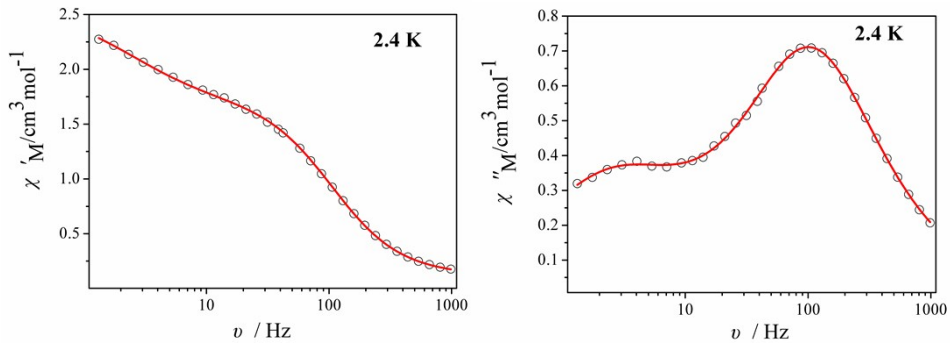


Figure S8. Frequency dependence of the in-of-phase (χ' , right) and out-of-phase (χ'' , left) ac susceptibility of **2** at 2.4 K. The full range plots can be fitted well by the following parameters: $\alpha_1 = 0.204$; $\alpha_2 = 0.105$; $\tau_1 = 1.48 \times 10^{-3}$ s; $\tau_2 = 0.066$ s; $\chi_{S,\text{tot}} = 0.111 \text{ cm}^3 \text{mol}^{-1}$; $\Delta\chi_1 = 1.585 \text{ cm}^3 \text{mol}^{-1}$; $\Delta\chi_2 = 0.864 \text{ m}^3 \text{mol}^{-1}$. The red lines are the fits of the full range plots.

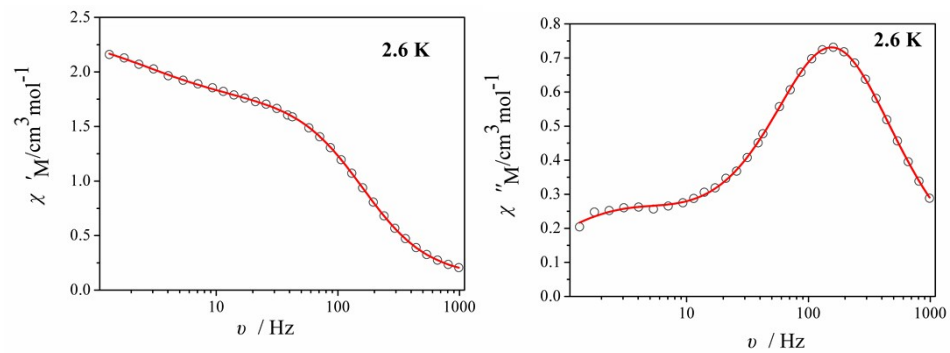


Figure S9. Frequency dependence of the in-of-phase (χ' , right) and out-of-phase (χ'' , left) ac susceptibility of **2** at 2.6 K. The full range plots can be fitted well by the following parameters: $\alpha_1 = 0.255$; $\alpha_2 = 0.091$; $\tau_1 = 9.91 \times 10^{-4}$ s; $\tau_2 = 0.061$ s; $\chi_{S,\text{tot}} = 0.106 \text{ cm}^3 \text{mol}^{-1}$; $\Delta\chi_1 = 1.626 \text{ cm}^3 \text{mol}^{-1}$; $\Delta\chi_2 = 0.649 \text{ cm}^3 \text{mol}^{-1}$. The red lines are the fits of the full range plots.

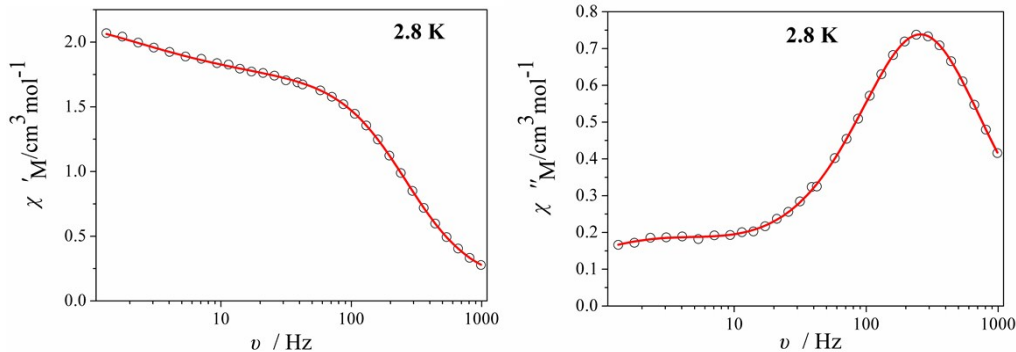


Figure S10. Frequency dependence of the in-of-phase (χ' , right) and out-of-phase (χ'' , left) ac susceptibility of **2** at 2.8 K. The full range plots can be fitted well by the following parameters: $\alpha_1 = 0.311$; $\alpha_2 = 0.073$; $\tau_1 = 6.04 \times 10^{-4}$ s; $\tau_2 = 0.07$ s; $\chi_{S,\text{tot}} = 0.106 \text{ cm}^3 \text{mol}^{-1}$; $\Delta\chi_1 = 1.614 \text{ cm}^3 \text{mol}^{-1}$; $\Delta\chi_2 = 0.558 \text{ cm}^3 \text{mol}^{-1}$. The red lines are the fits of the full range plots.

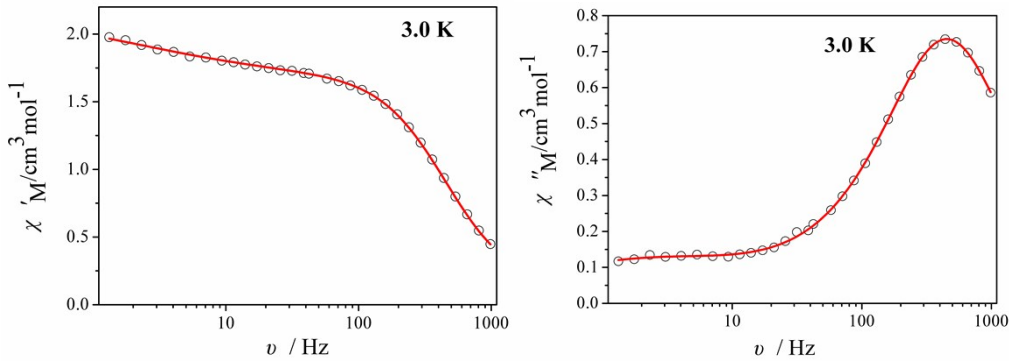


Figure S11. Frequency dependence of the in-of-phase (χ' , right) and out-of-phase (χ'' , left) ac susceptibility of **2** at 2.6 K. The full range plots can be fitted well by the following parameters: $\alpha_1 = 0.428$; $\alpha_2 = 0.059$; $\tau_1 = 3.46 \times 10^{-4}$ s; $\tau_2 = 0.073$ s; $\chi_{S,\text{tot}} = 0.105 \text{ cm}^3 \text{mol}^{-1}$; $\Delta\chi_1 = 1.576 \text{ cm}^3 \text{mol}^{-1}$; $\Delta\chi_2 = 0.485 \text{ cm}^3 \text{mol}^{-1}$. The red lines are the fits of the full range plots.

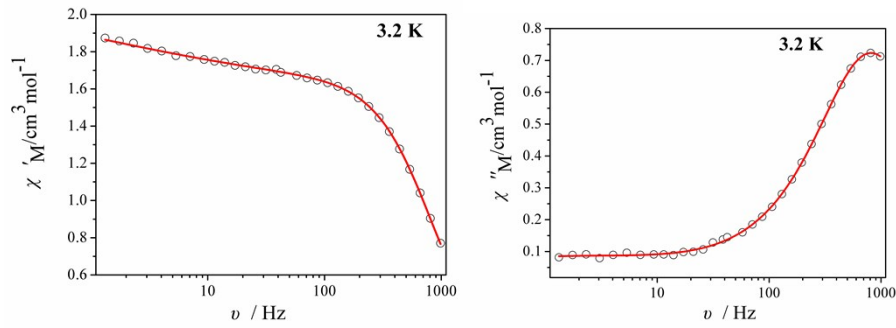


Figure S12. Frequency dependence of the in-of-phase (χ' , right) and out-of-phase (χ'' , left) ac susceptibility of **2** at 3.2 K. The full range plots can be fitted well by the following parameters: $\alpha_1 = 0.429$; $\alpha_2 = 0.044$; $\tau_1 = 1.93 \times 10^{-4}$ s; $\tau_2 = 0.11$ s; $\chi_{S,\text{tot}} = 0.105 \text{ cm}^3 \text{mol}^{-1}$; $\Delta\chi_1 = 1.509 \text{ cm}^3 \text{mol}^{-1}$; $\Delta\chi_2 = 0.49 \text{ cm}^3 \text{mol}^{-1}$. The red lines are the fits of the full range plots.

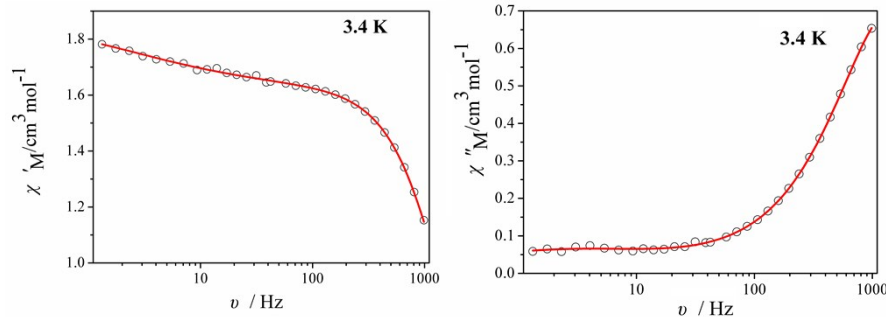


Figure S13. Frequency dependence of the in-of-phase (χ' , right) and out-of-phase (χ'' , left) ac susceptibility of **2** at 3.4 K. The full range plots can be fitted well by the following parameters: $\alpha_1 = 0.437$; $\alpha_2 = 0.069$; $\tau_1 = 9.87 \times 10^{-5}$ s; $\tau_2 = 0.062$ s; $\chi_{S,\text{tot}} = 0.039 \text{ cm}^3 \text{mol}^{-1}$; $\Delta\chi_1 = 1.585 \text{ cm}^3 \text{mol}^{-1}$; $\Delta\chi_2 = 0.258 \text{ cm}^3 \text{mol}^{-1}$. The red lines are the fits of the full range plots.

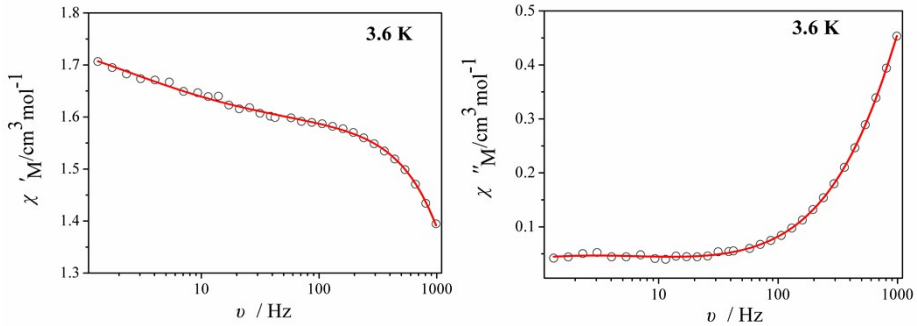
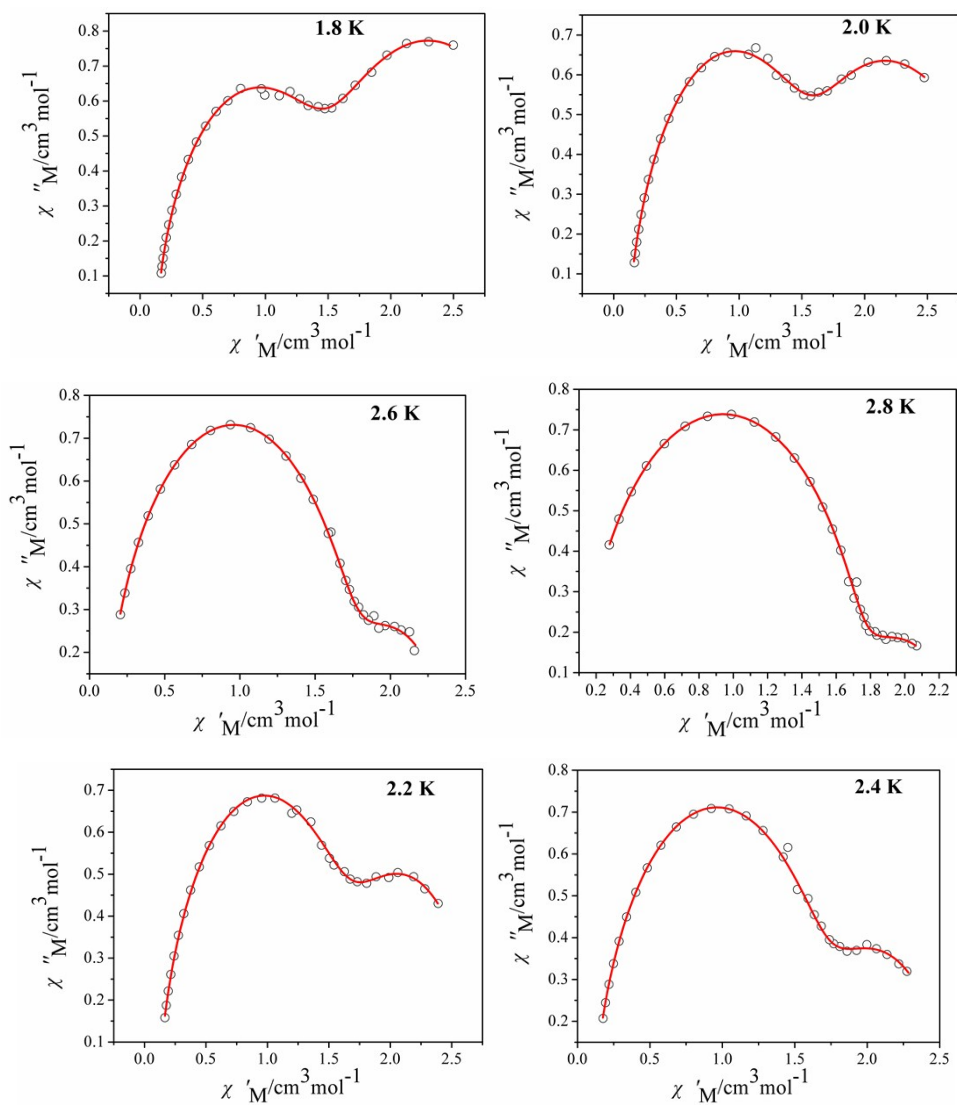


Figure S14. Frequency dependence of the in-of-phase (χ' , right) and out-of-phase (χ'' , left) ac susceptibility of **2** at 3.6 K. The full range plots can be fitted well by the following parameters: $\alpha_1 = 0.455$; $\alpha_2 = 0.106$; $\tau_1 = 3.82 \times 10^{-5}$ s; $\tau_2 = 0.074$ s; $\chi_{S,\text{tot}} = 0.089 \text{ cm}^3\text{mol}^{-1}$; $\Delta\chi_1 = 1.927 \text{ cm}^3\text{mol}^{-1}$; $\Delta\chi_2 = 0.194 \text{ cm}^3\text{mol}^{-1}$. The red lines are the fits of the full range plots.



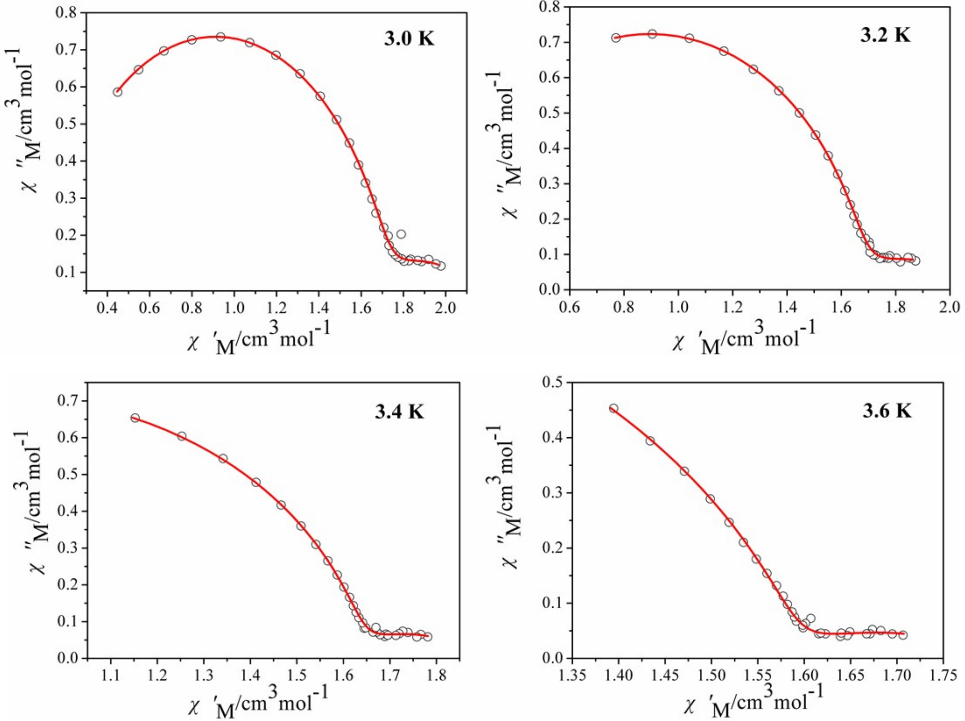


Figure S15. Simulations of dynamical susceptibility $\chi(\omega)$ ranging from 1.8 to 3.6 K in a Cole-Cole diagram of **2**. Red lines were performed using the sum of two modified Debye functions with the fitting parameters in Table S5. The magnetic susceptibility data were described by the sum of two modified Debye functions:

$$\chi''(\omega) = \Delta\chi_1 \frac{(\omega\tau_1)^{1-\alpha_1} \cos(\pi\alpha_1/2)}{1 + 2(\omega\tau_1)^{1-\alpha_1} \sin(\pi\alpha_1/2) + (\omega\tau_1)^{(2-2\alpha_1)}} + \Delta\chi_2 \frac{(\omega\tau_2)^{1-\alpha_2} \cos(\pi\alpha_2/2)}{1 + 2(\omega\tau_2)^{1-\alpha_2} \sin(\pi\alpha_2/2) + (\omega\tau_2)^{(2-2\alpha_2)}}$$

$\Delta\chi_1, \tau_1, \alpha_1, \Delta\chi_2, \tau_2, \alpha_2$

$$\chi'(\omega) = \chi_{S,\text{tot}} + \Delta\chi_1 \frac{1 + (\omega\tau_1)^{1-\alpha_1} \sin(\pi\alpha_1/2)}{1 + 2(\omega\tau_1)^{1-\alpha_1} \sin(\pi\alpha_1/2) + (\omega\tau_1)^{(2-2\alpha_1)}} + \Delta\chi_2 \frac{1 + (\omega\tau_2)^{1-\alpha_2} \sin(\pi\alpha_2/2)}{1 + 2(\omega\tau_2)^{1-\alpha_2} \sin(\pi\alpha_2/2) + (\omega\tau_2)^{(2-2\alpha_2)}}$$

$\chi_{S,\text{tot}}, \Delta\chi_1, \tau_1, \alpha_1, \Delta\chi_2, \tau_2, \alpha_2$

Table S6. Relaxation fitting parameters from Least-Squares Fitting of $\chi(\omega)$ data of **2**.

T(K)	$\chi_{S,\text{tot}}(\text{cm}^3\text{mol}^{-1})$	$\Delta\chi_1(\text{cm}^3\text{mol}^{-1})$	$\Delta\chi_2(\text{cm}^3\text{mol}^{-1})$	α_1	α_2	$\tau_1(\text{s})$	$\tau_2(\text{s})$
1.8	0.137	1.872	1.322	0.169	0.126	2.85×10^{-3}	0.104
2.0	0.122	1.493	1.419	0.174	0.13	2.49×10^{-3}	0.084
2.2	0.115	1.556	1.077	0.156	0.131	2.08×10^{-3}	0.069
2.4	0.111	1.585	0.864	0.204	0.105	1.48×10^{-3}	0.066
2.6	0.106	1.626	0.649	0.255	0.091	9.91×10^{-4}	0.061
2.8	0.106	1.614	0.558	0.331	0.073	6.04×10^{-4}	0.07
3.0	0.105	1.576	0.485	0.428	0.059	3.46×10^{-4}	0.073
3.2	0.105	1.509	0.49	0.429	0.044	1.93×10^{-4}	0.11
3.4	0.039	1.585	0.258	0.437	0.069	9.87×10^{-5}	0.062
3.6	0.089	1.927	0.194	0.455	0.106	3.82×10^{-5}	0.074